

# FREE SURFACE CRACKING DUE TO PITTING AND ROLLING

C. H. Chue and H. H. Chung

Department of Mechanical Engineering, National Cheng Kung University Tainan, Taiwan 70101

## ABSTRACT

The mechanism of pitting caused by rolling contact is analyzed using the fracture mechanics approach. The governing factors are the initial crack length, crack angle, contact force, friction, strain-hardened layer, and the hydraulic pressure of trapped fluid acting on the crack surface. The strain energy density factors are calculated by application of the two-dimensional finite element method. The strain energy density criterion is applied to show that shallow angle crack under small rolling contact force and friction enhances the probability of pitting under the roller's running surface. The presence of a strain hardened surface layer also tends to affect the fracture behavior. The analytical results agree well with the experimental observations.

## 1 INTRODUCTION

Rolling contact problem involving cracks has had a long standing interest. Stress intensity factor calculations have been made [1] for two-dimensional surface-breaking cracks under Hertzian contact stress distribution. The complex variable technique was used [2] to solve the two-dimensional problem of a rigid cylinder sliding on an elastic half-space with a surface-breaking crack. Discussed in [3-6] are the growth mechanism of surface-breaking cracks in elastic half-space subjected to repeat loading. The pressure created by the fluid tends to enhance crack propagation and alter the direction of growth [7]. Despite the great number of past investigations, the phenomena of crack initiation and propagation associated with rolling contact are still not fully understood.

## 2 PROBLEM STATEMENT

Figure 1 depicts a circular cylindrical on an elastic plate of length  $W = 1.5$  mm and the thickness  $H = 0.55$  mm which will be treated as an elastic half-space. The Young's modulus and Poisson's ratio of the elastic plate are 282 GPa and 0.3, respectively. The crack makes an angle  $\beta$  with the surface in the rolling  $x$ - direction. The rigid cylinder of radius  $R$  indents the plate surface with depth  $d$ . It runs at a velocity  $V = 0.0838$  mm/sec and rotates at an angular velocity  $\omega = 0.01$  radian/sec from  $x = -0.2$  mm to the  $x = 0.3028$  mm. The bottom of the plate is fixed and the two sides are allowed to move only in the  $y$ - direction. Note that  $h$  denotes the thickness of the strain-hardened layer

## 3 RESULTS AND DISCUSSIONS

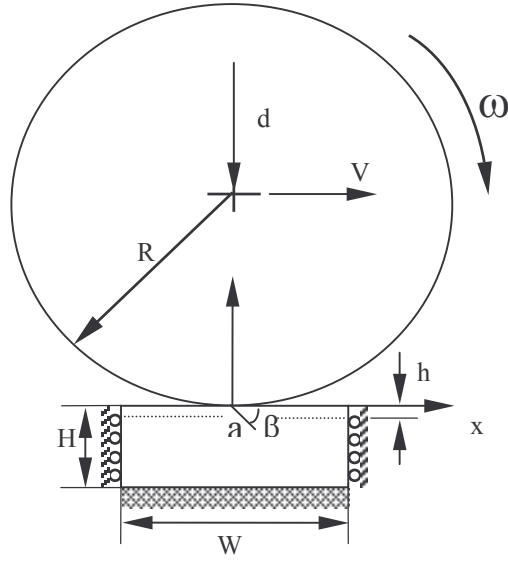


Figure 1. Schematic of rigid circular roller on cracked plate.

### 3.1 Critical pressure

It is of interest to define the critical pressure  $p_{cr}$  at which pitting will initiate. Shown in Figure 2 are the variations of  $S_{min}$  for  $a = 0.06$  mm,  $\beta = 25^\circ$ ,  $\mu = 0.05$  and  $d = 0.006$  mm. The maximum of  $S_{min}$  occurs at A. According to the minimum strain energy density theory [8], the crack would initiate, say in the direction  $\theta_0$  when the maximum  $S_{min}$  reaches  $S_C$  for the given material. If the analysis is continued until the crack grows from  $a = 0.012$ mm, the final configuration corresponds to that given in Figure 3(a) for  $p = 650$  MPa. A pit near the surface is thus formed. Suppose that  $S_{min}$  reaches  $S_C$  at B in Fig. 2, the crack path would correspond to that shown in Figure 3(b) where it extends downward into the substrate. Both cases have been observed from experiments [11]. The corresponding pressure  $p$  is defined as the “critical pressure”  $p_{cr}$ .

### 3.2 Indentation force

By specifying the downward displacement of the rigid roller, an indentation force exerted by roller can be computed. For  $a = 0.012$  mm and  $\beta = 25^\circ$ , Figure 4 shows a relation between the critical hydraulic pressure  $p_{cr}$  and indentation depth  $d$ . Each point at the curve predicts pitting. The corresponding critical pressure  $p_{cr}$  tends to increase with the indentation depth.

### 3.3 Initial crack length and position

Figure 5 displays the variations of the critical pressure  $p_{cr}$  with the initial crack length for different crack angles  $\beta$ . It shows that short crack length  $a$  and small crack angle  $\beta$  correspond to lower hydraulic pressure for creating a pit. If the initial crack length is long and/or the initial crack angle is large, the crack would extend downward.

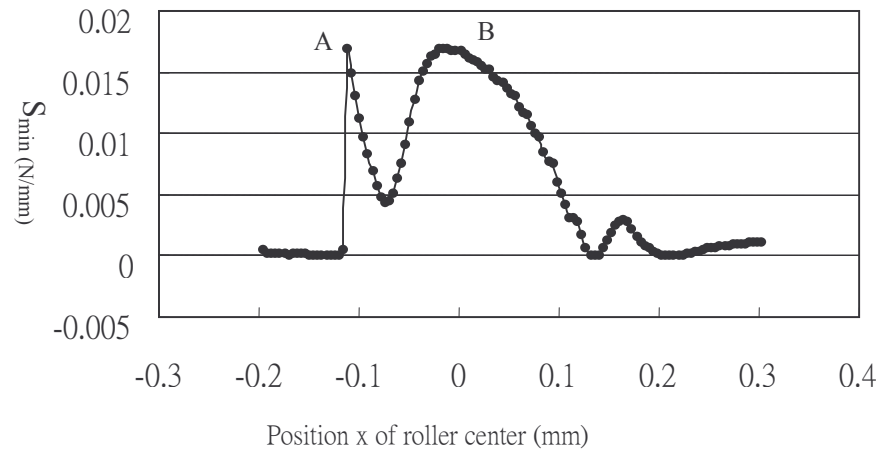


Figure 2. Variations of minimum strain energy density factor with roller center for  $a = 0.06$  mm,  $\beta$

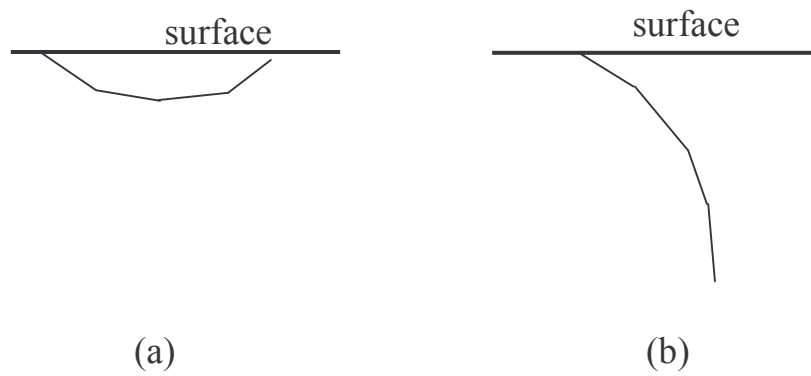


Figure 3. Step-by-step finite element results of crack path for  $a = 0.012$  mm,  $\beta = 25^\circ$ ,  $\mu = 0.05$  and  $d = 0.006$  mm (a)  $p = 650$  MPa, (b)  $p = 450$  MPa.

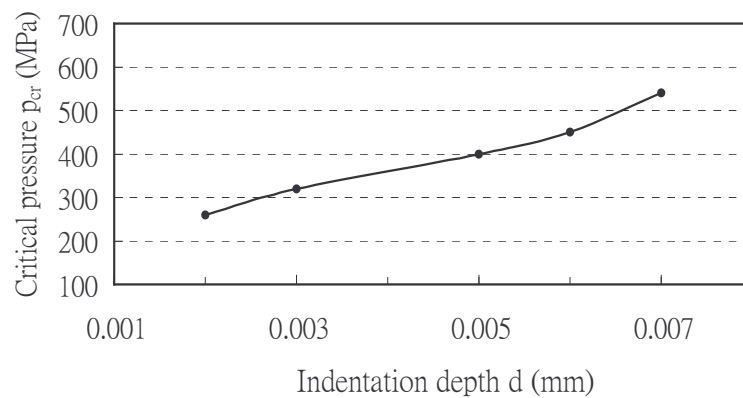


Figure 4. Variations of critical pressure with indentation depth for  $a = 0.012$  mm,  $\beta = 25^\circ$  and  $\mu = 0.05$ .

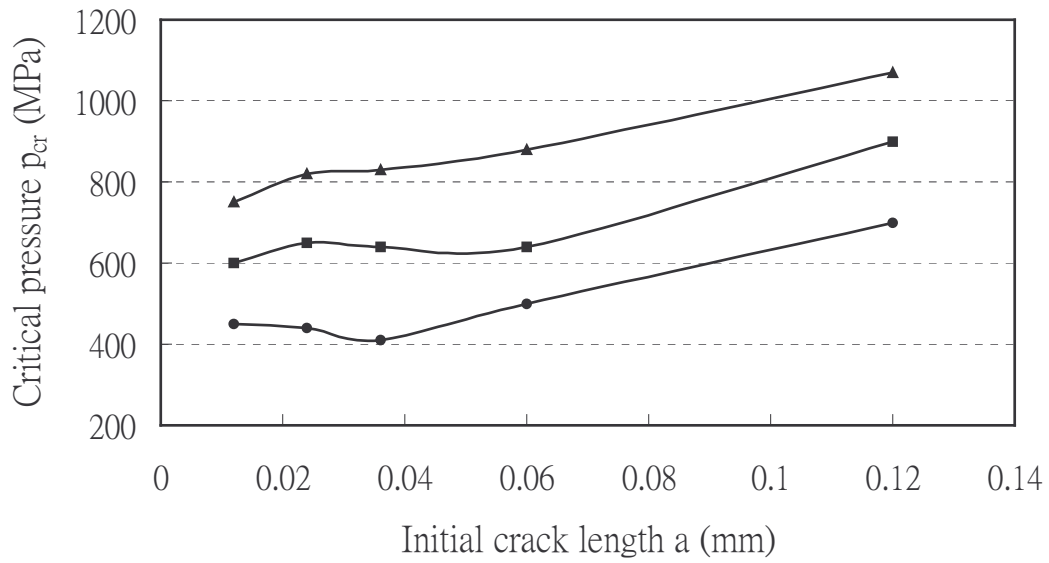


Figure 5. Critical pressure versus initial crack length for different crack angles  $\beta$  with  $\mu = 0.05$  and  $d = 0.006$  mm.

### 3.4 Coefficient of friction

Figure 6 shows a plot of critical pressure  $p_{cr}$  against the coefficient of friction for  $a = 0.012$  mm,  $\beta = 25^\circ$  and  $d = 0.006$  mm. For dry rollers with high  $\mu$  [7], pits did not form. Pit formation was rapid in good lubricant conditions where friction was low.

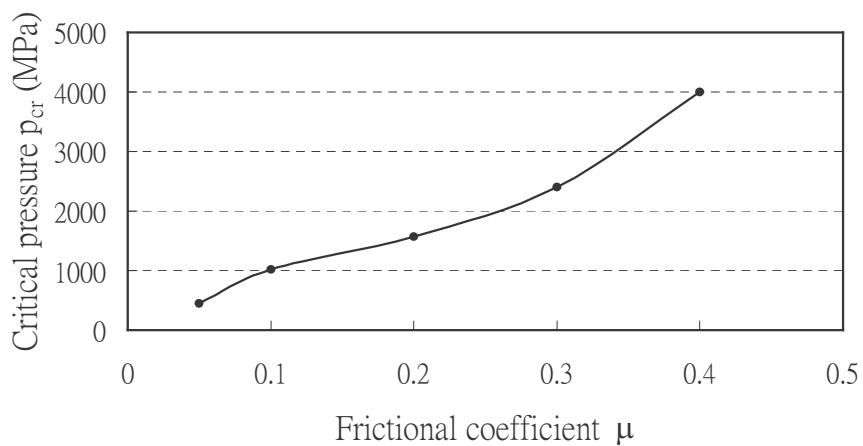


Figure 6. Critical pressure versus coefficient of friction for  $a = 0.012$  mm,  $\beta = 25^\circ$  and  $d = 0.006$  mm.

### 3.5 Strain-hardened surface layer

A strain hardened surface layer is formed under repeated application of elastic-plastic stress arising from rolling contact. For layer thickness  $h$  equal to 0.01 mm and a Young's modulus 1.4 times that of the base plate material,  $\beta = 25^\circ$  and  $d = 0.006$  mm, Figure 7 gives the critical pressure as a function of the initial crack length for different  $\mu$ . For steeply inclined cracks with  $a = 0.012$  mm and 0.024 mm, the tips are in the layer. Hence, higher critical pressure would be required to form a pit on account of the hardened layer. Moreover, higher coefficient of friction tends to enhance downward crack growth.

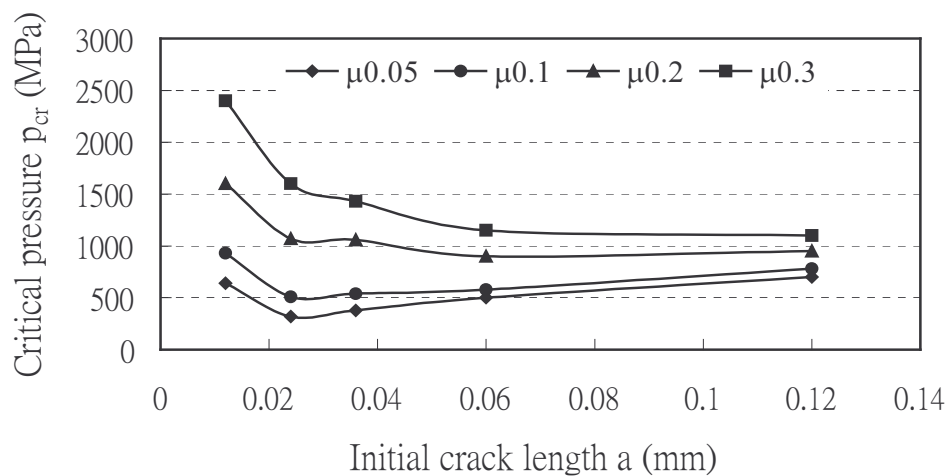


Figure 7. Critical pressure versus initial crack length for different  $\mu$  with  $\beta = 25^\circ$ ,  $d = 0.006$  mm and  $h = 0.01$  mm.

### 5 REFERENCES

- [1] L. M. Keer, M. D. Bryant, A pitting model for rolling contact fatigue, ASME J. Lubrication Technology 105 (1983) 198-205.
- [2] M. D. Bryant, G. R. Miller, L. M. Keer, Line contact between a rigid indenter and a damaged elastic body, Q. JI Mech. Appl. Math. 37 (3) (1984) 467-478.
- [3] M. Kaneta, H. Yatsuzuka, Y. Murakami, Mechanism of crack growth in lubricated rolling/sliding contact, ASLE Trans. 28 (3) (1985) 407-414.
- [4] Y. Murakami, M. Kaneta, H. Yatsuzuka, Analysis of surface crack propagation in lubricated rolling contact, ASLE Trans. 28 (2) (1985) 60-68.
- [5] M. Kaneta, Y. Murakami, Effects of oil hydraulic pressure on surface crack growth in rolling/sliding contact, Tribology Int. 20 (4) (1987) 210-217.
- [6] Y. Murakami, C. Sakae, K. Ichimaru, Three-dimensional fracture mechanics analysis of pit formation mechanism under lubricated rolling-sliding contact load, STLE Tribology Trans. 37 (3) (1994) 445-454.

- [7] S. Way, Pitting due to rolling contact, ASME J. Appl. Mech. 2 (1935) A49-A58.
- [8] G. C. Sih, Strain-energy-density factor applied to mixed mode crack problems, Int. J. Fract. 10 (1974) 305-321.
- [9] C. C. Chou, Tribological effects of surface roughness and EP additive on the run-in process and pitting behavior of oil-lubricated line contacts, Ph.D. dissertation, Department of Mechanical Engineering, National Cheng Kung University, 1998.